Low-temperature photoluminescence of WSe$_2$ monolayer obtained by gold-assisted exfoliation

© *S.N. Nikolaev, V.S. Bagaev, M.A. Chernopitssky, I.I. Usmanov, E.E. Onishchenko, A.A. Deeva, V.S. Krivobok*

Lebedev Physical Institute, Russian Academy of Sciences,
119991 Moscow, Russia

E-mail: nikolaev-s@yandex.ru

We studied the optical properties of an atomically thin WSe$_2$ film obtained by gold-assisted mechanical exfoliation. Raman scattering spectra, low-temperature photoluminescence, and micro-reflection from large-scale monolayer are investigated. At room temperature, the optical properties of such a film reproduce the properties of WSe$_2$ monolayers obtained by regular mechanical exfoliation. It is shown that at low temperatures, the radiation spectra of the resulting film are determined by standard mechanisms of radiative recombination involving free excitons, bound excitons, and trions. However, in contrast to room temperatures, there is a significant difference in the spectral width and intensity of the lines compared to monolayers WSe$_2$, obtained regular way from the same source material. The differences found, demonstrating a significant increase in background doping and structural disorder when using gold-assisted exfoliation, may be meaningful for a number of optoelectronic applications of atomically thin WSe$_2$ films.

Keywords: layered semiconductors, luminescence, monolayer, escitons.

1. Introduction

Transition metal dichalcogenides (TMD) are classified as laminates that have attracted interest over the past few years owing to their electrical and mechanical properties and wide heterostructure engineering capabilities [1,2]. Layers in TMD are held together by low Van der Waals (VDW) forces that allow separation into monolayers (a single whole containing three atomic planes — one plane with transition metal atoms sandwiched between two chalcogen atom planes). Monolayers of many TMD such as MoS$_2$, WS$_2$, WSe$_2$ and MoSe$_2$ are of particular interest because they are semiconductors with direct bandgap [3,4], what makes them promising materials for several modern optoelectronics applications.

Mechanical exfoliation using an duct tape so called „top-down" technique is the most common monolayer production technology [5]. 1 monolayer thick TMD films produced by a traditional mechanical exfoliation technique have a small lateral size ($\sim 5\,\mu$m). In addition, the exfoliation process is rather difficult to be controlled and probability of producing monolayers is low. Some time ago, it was demonstrated that both lateral dimension and monolayer production probability during mechanical exfoliation of VDW materials may be increased dramatically by gold film sputtering [6]. Such approach is enabled due to the fact that gold has strong affinity with chalcogens with which it forms a homopolar bond. However, notwithstanding the successful production of relatively large monolayers using this method, their structural and optical properties have been scarcely addressed.

Optical properties analysis of atomically thin WSe$_2$ film produced with the use of gold is discussed herein. It is shown herein that optical properties of such film are specific to typical WSe$_2$ monolayers at room temperature. At the same time, photoluminescence spectra (PL) of the film obtained using gold at helium temperature differ drastically from those of the monolayers obtained by a „traditional" technology. The observed differences associated both with an obvious increase in background doping and consolidation of the structural disorder role may be significant for a wide range of optoelectronic applications of atomically thin WSe$_2$ films.

2. Production procedure and preliminary characterization

The test sample was prepared by gold-assisted splitting of WSe$_2$ bulk crystal. Then, it was transferred onto SiO$_2$/Si substrate with a 300 nm oxide layer. Gold is known to have strong affinity with chalcogens with which it forms a homopolar bond. The production process for lamellar semiconductor thin layers with large lateral dimension is schematically shown on Fig. 1. Using a thermoresistive method, gold is sputtered on a WSe$_2$ bulk crystal applied onto an duct tape. Gold atoms are bonded with chalcogen atoms in the uppermost layer of the bulk crystal. Interaction between the top layer and gold is stronger than Van der Waals interaction with WSe$_2$ bottom layers. This enables selective exfoliation of the top layer using a thermal release tape that is subsequently transferred onto the SiO$_2$/Si substrate. Then the thermal release tape shall be removed
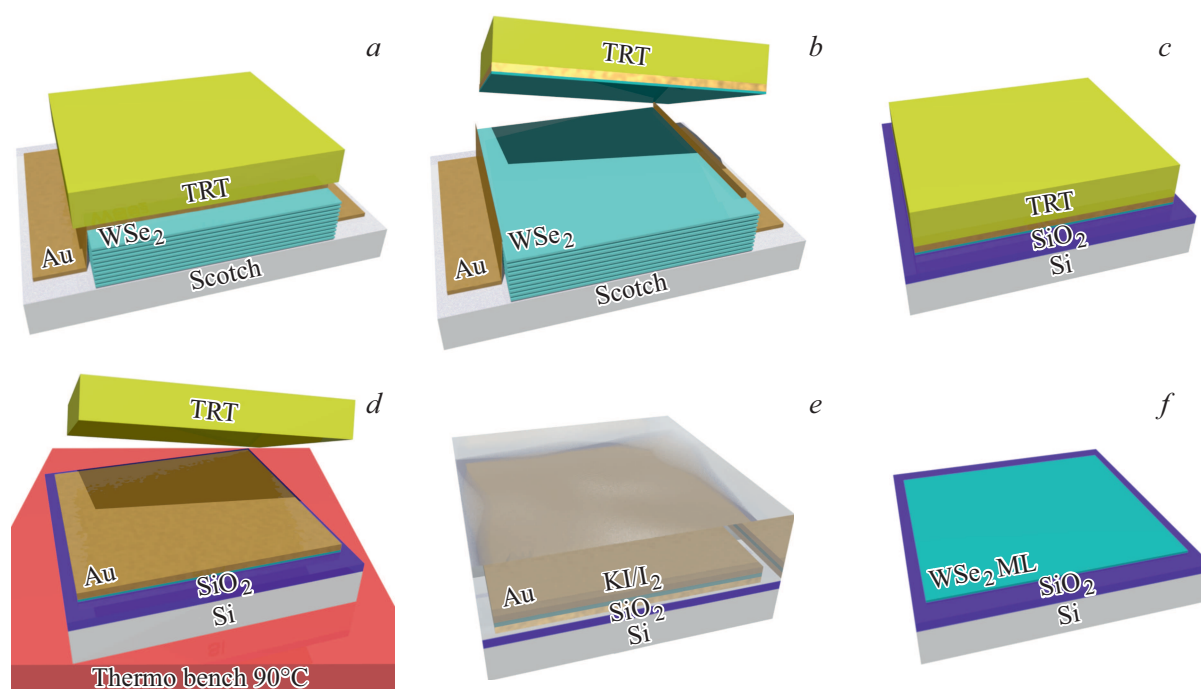
Figure 1. Production of laterally large monolayers of lamellar semiconductors: *a* — a bulk crystal is applied onto a duct tape, gold sputtered and engaged with a thermal release tape; *b* — the thermal release tape is removed together with the gold film and top layer of the bulk crystal; *c* — the thermal release tape with the monolayer is transferred to a target substrate; *d* — the thermal release tape is removed by heating up to 90°C on a hot bench; *e* — the gold film is etched away in KI/I$_2$ solution; *f* — the substrate with the monolayer is finally cleaned at the last step.
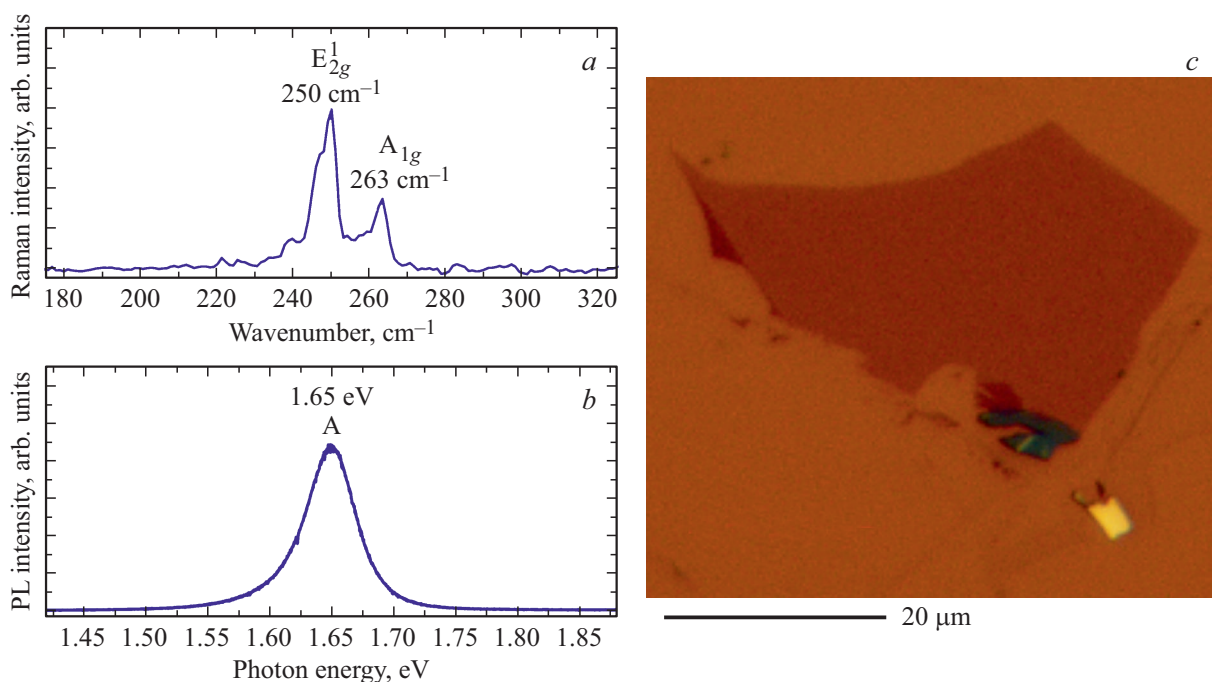

Figure 2. *a* is a Raman scattering spectrum at excitation wavelength 532 nm; *b* is a photoluminescence spectrum at room temperature; *c* is the image of the produced monolayer WSe$_2$.

by heating up to 90°C on a hot bench, and the substrate is treated in oxygen plasma to remove the remaining tape from the surface. At the next step, the gold film is etched with potassium iodide (KI). The last step involves cleaning with acetone, isopropyl alcohol and distilled water to remove the remaining adhesive.

Relatively strong bonding between gold and uppermost WSe₂ layer enhanced the probability of crystal splitting exactly in the uppermost layer and, thus, it will be possible to obtain a monolayer whose dimensions will be technically limited only by the initial crystal. Figure 2, *c* shows a light-microscopical image of the obtained WSe₂ monolayer. The layer dimensions are approx. $\sim 20 \times 30\,\mu\text{m}$. The layer thickness of $\sim 1\,\text{nm}$ was verified by atomic-force microscopy.

Figure 2, *a* shows a Raman scattering spectrum of the prepared sample at room temperature. Two peaks in the area of 250 and 263 cm⁻¹ were observed during the Raman scattering experiment. It is known from [7] that the peak at 250 cm⁻¹ is caused by E_{2g}^1 phonon mode, and the peak at 263 cm⁻¹ corresponds to A_{1g} mode. The absence of signal at 310 cm⁻¹ assigned to B_{2g}^1 vibrational mode proves that the obtained sample is a monolayer. The photoluminescence spectrum (Fig. 2, *b*) at room temperature has a single line with photon energy 1.65 eV. The peak position and halfwidth definitely associate the peak with direct-band A exciton that is the main state in one monolayer thick WSe₂ films [8].

3. Low-temperature photoluminescence of WSe₂ monolayer

For purpose of investigations of the low-temperature photoluminescence, the sample was placed in Utreks continuous-flow helium cryostat with the operating temperature range of 5−300 K. Optical excitation and sample emission acquisition were performed in a confocal scheme. Laser emission was focused on the sample surface into a 2−3 μm spot using a microlens placed in the cryostat together with the sample. For laser beam focus adjustment, a 4f-scanner scheme was used. Cobolt Samba 532 nm continuous-wave laser was used for excitation. Photoluminescence emission, Raman scattering and sample microreflections were examined using Acton 2500 grating spectrometer and recorded by PyLoN 100B cooled CCD sensor.

Figure 3 shows PL spectra of three WSe₂ monolayers, one of which was produced using a technique mentioned above. The spectral lines of WSe₂ monolayers on SiO₂/Si with energies 1.745 and 1.715 eV are assigned to A-excitons and negatively charged T⁻ trions [9], and lines within 1.6−1.7 eV are assigned to fault-bound states [10] or multiparticle states [11]. It can be seen that there are no significant changes in spectral position of the exciton and trion lines. At the same time, their width was considerably increased when gold was used. In the gold-assisted film spectrum, a trion emission line is dominating which is indicative of an increase in the free electron density in it. The relationship between the free and bound exciton line intensities has a weak dependence on the film production method, however, widening of the localized state lines does not allow to enable them now.
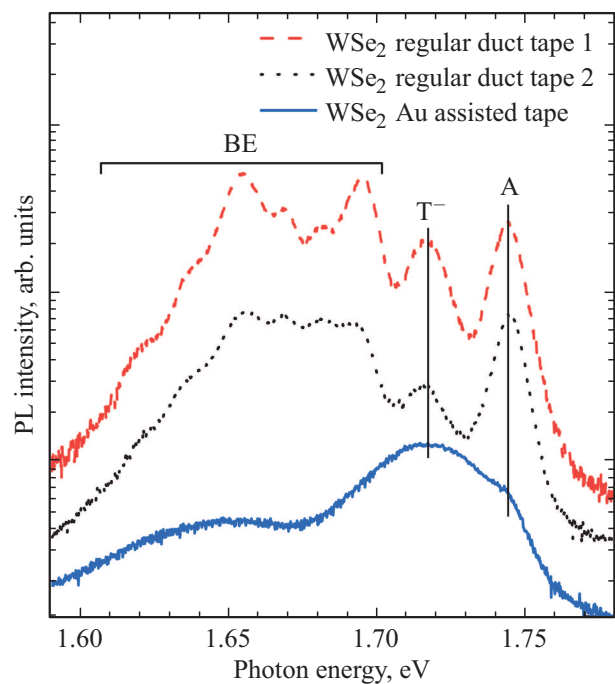

Figure 3. Comparison of low-temperature (5 K) photoluminescence of WSe₂ monolayers produced using a regular duct tape and WSe₂ monolayer produced by gold-assisted micromechanical exfoliation method.

The relationship of microreflection spectra recorded at 5 K from the SiO₂/Si substrate regions with and without WSe₂ monolayer is shown in Fig. 4, *a*. These spectra that illustrate small changes in the reflection spectrum in the region containing the monolayer demonstrate the appearance of a resonant feature within 1.68−1.80 eV. This feature was caused by sharp change in the dielectric function of WSe₂ close to the main bright exciton state [12]. For sequential analysis of the feature, reflection spectra shall be simulated, however, the spectral position of the main exciton resonance may be assessed from the „center-of-gravity" position of the resonant feature. As shown in Fig. 4, *a*, it is located in the area of ~ 1.745 eV, which corresponds to A-line in the photoluminescence spectra.

Thus, the measurements of microreflection spectra from the gold-assisted monolayer demonstrate that A-line is associated exactly with the main (bright) exciton resonance.

Figure 4, *b* shows photoluminescence spectra vs. 472 nm laser emission excitation power density. It can be clearly seen in the figure that the spectrum structure, including three main lines, is virtually unchanged with the change in optical pumping at least by a factor of 2. This means that the differences observed in Fig. 3 are an artifact caused by different excitation power density and/or a change in the nonradiative recombination rate.

The band intensity grows with power density superlinearly $\sim P^{1.2}$. For WSe₂ monolayers, the superlinear growth of exciton luminescence intensity at low temperatures is
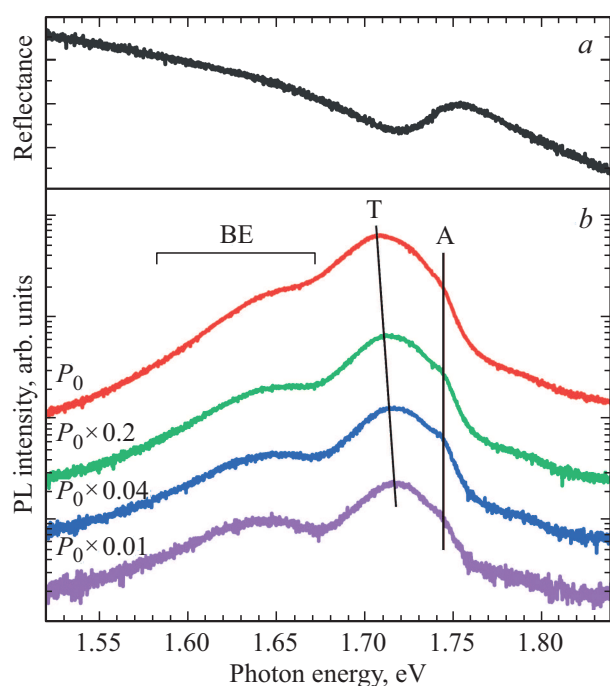
Figure 4. *a* is the microreflection spectrum of WSe$_2$ monolayer; *b* is the low-temperature (5 K) photoluminescence spectra vs. laser excitation power density $P_0 = 32\,\text{kW/cm}^2$.

generally explained by the need in population of bright exciton states by Augerprocesses. Since for Augerprocesses, interaction between three and more nonequilibrium carriers is required, their rate grows sharply with the excitation power density. However, for undoped (inherent) WSe$_2$, where exciton states prevail, this dependence shall be close to quadratic. The superlinear dependence with exponent ~ 1.2 shows that the main Auger-processes populating the bright exciton states are characterized by collisions involving excitons and nonequilibrium carriers. Moreover, concentration of the latter is considerably higher than the concentration of excitons generated by optical excitation. This feature of the gold-assisted monolayer proves that it contains a significant concentration of carriers of the same sign. Since T$^-$-trion is the brightest line in the emission spectra, electrons serve as such carriers.

The experimental data shown in Figs. 3, 4 prove the increase in film heterogeneity accompanied by a surface density growth of conductivity electrons in it. It is known that the chalcogen vacancies in DCM films are the main fault leading to *n*-type conductivity [13]. In addition, these faults are the centers of oxygen and water absorption from atmosphere which will lead to a change in the dielectric environment near the vacancies in the film. Therefore, the found differences between the luminescence spectra of monolayers obtained using the traditional technique and the gold-assisted technique shall be preliminary assigned to the increase in Se vacancy density.

4. Conclusion

Thus, the micromechanical exfoliation using gold film enabled to obtain atomically thin WSe$_2$ layer with a lateral dimension of $\sim 20 \times 30\,\mu$m. The layer was characterized using optical contrast microscopy, Raman scattering spectra measurement, reflection and low-temperature photoluminescence. It is shown that optical properties at room temperature do not differ from that of WSe$_2$ monolayers produced by the traditional mechanical exfoliation method. At helium temperatures in photoluminescence spectra of the obtained layer, a wide band with 1.715 eV maximum dominates and is associated with the radiative recombination of negatively charged trions. On its short-wave and long-wave wings, less intensive emission lines are recorded associated with recombination of free (~ 1.745 eV) and bound (1.65 eV) excitons, respectively. Despite the typical positions of the main lines, their relative intensities and widths differ drastically from that of WSe$_2$ monolayers obtained by a traditional method from the same material. The observed differences indicate that the gold-assisted mechanical exfoliation facilitates the increased role of structural disorder and additional electron injection, apparently, due to chalcogen vacancy generation.

Conflict of interest

The authors declare that they have no conflict of interest.

References

[1] A. Chaves, J.G. Azadani, H. Alsalman, D.R. da Costa, R. Frisenda, A.J. Chaves, S.H. Song, Y.D. Kim, D. He, J. Zhou, A. Castellanos-Gomez, F.M. Peeters, Zheng Liu, C.L. Hinkle, Sang Hyun Oh, Peide D. Ye, S.J. Koester, Young Hee Lee, Ph. Avouris, Xinran Wang. npj 2D Mater. Appl., **4** (1), 29 (2020).

[2] D. Waters, Y. Nie, F. Luüpke, Y. Pan, S. Fölsch, Y.-C. Lin, B. Jariwala, K. Zhang, C. Wang, H. Lv, K. Cho, D. Xiao, J.A. Robinson, R.M. Feenstra. ACS Nano, **14** (6), 7564 (2020).

[3] K.F. Mak, C. Lee, J. Hone, J. Shan, T.F. Heinz. Phys. Rev. Lett., **105** (13), 136805 (2010).

[4] W. Zhao, Z. Ghorannevis, L. Chu, M. Toh, C. Kloc, P.-H. Tan, G. Eda. ACS Nano, **7** (1), 791 (2013).

[5] K.S. Novoselov, A.K. Geim, S.V. Morozov, D. Jiang, Y. Zhang, S.V. Dubonos, I.V. Grigorieva, A.A. Firsov. Science, **306** (5696), 666 (2004).

[6] Z. Lin, A. Mc Creary, N. Briggs, S. Subramanian, K. Zhang, Y. Sun, X. Li, N. J. Borys, H. Yuan, S.K. Fullerton-Shirey, A. Chernikov, H. Zhao, St. Mc Donnell, A.M. Lindenberg, K.Xiao, B.J. Le Roy, M. Drndic, J. CM Hwang, J. Park, M. Chhowalla, R.E. Schaak, A. Javey, M.C. Hersam, J. Robinson, M. Terrones. 2D Materials, **3** (4), 042001 (2016).

[7] X. Luo, Y. Zhao, J. Zhang, M. Toh, C. Kloc, Q. Xiong, S.Y. Quek. Phys. Rev. B, **88** (19), 195313 (2013).

[8] W. Zhao, R.M. Ribeiro, M. Toh, A. Carvalho, C. Kloc, A.H. Castro Neto, G. Eda. Nano Lett., **13** (11), 5627 (2013).

[9] G. Wang, L. Bouet, D. Lagarde, M. Vidal, A. Balocchi, T. Amand, X. Marie, B. Urbaszek. Phys. Rev. B, **90** (7), 075413 (2014).

[10] S. Tongay, J. Suh, C. Ataca, W. Fan, A. Luce, J.S. Kang, J. Liu, C. Ko, R. Raghunathanan, J. Zhou, F. Ogletree, J. Li, J.C. Grossman, J. Wu. Sci. Rept., **3** (1), 2657 (2013).

[11] Y. You, X.-X. Zhang, T.C. Berkelbach, M.S. Hybertsen, D.R. Reichman, T.F. Heinz. Nature Physics, **11** (6), 477 (2015).

[12] A. Arora, M. Koperski, K. Nogajewski, J. Marcus, C. Faugeras, M. Potemski. Nanoscale, **7** (23), 10421 (2015).

[13] W. Zhou, X. Zou, S. Najmaei, Z. Liu, Y. Shi, J. Kong, J. Lou, P.M. Ajayan, B.I. Yakobson, J.-C. Idrobo. Nano Lett., **13** (6), 2615 (2013).